Soft x-ray excited optical luminescence: Some recent applications

Y. F. Hu[a] and K. H. Tan
Canadian Synchrotron Radiation Facility, Synchrotron Radiation Center, University of Wisconsin-Madison, 3731 Schneider Drive, Stoughton, Wisconsin 53589

P. S. Kim, P. Zhang, S. J. Naftel, and T. K. Sham
Department of Chemistry, University of Western Ontario, London, Ontario, Canada N6A 5B7

I. Coulthard and B. W. Yates
Canadian Light Source, University of Saskatchewan, Saskatoon, SK, Canada S7N 5C6

(Presented on 22 August 2001)

X-ray excited optical luminescence (XEOL) studies of several classes of light emitting materials excited using soft x rays (photon energy ranging from 10 to 2500 eV) are presented. We show that XEOL with soft x rays (short penetration depths) is often site specific and is ideally suited for the study of light emitting thin films and devices. Several examples including porous silicon, organic light emitting diode materials, and CdS based nanostructures are used to illustrate the unique properties of XEOL and its applications in the soft x-ray energy region. © *2002 American Institute of Physics.* [DOI: 10.1063/1.1436540]

I. INTRODUCTION

X-ray absorption spectroscopy has been used extensively to study the electronic and structural properties of materials. X-ray absorption near edge structures (XANES) are especially useful in probing the unoccupied electronic states. XANES are typically measured in total electron yield (TEY) and/or fluorescence yield (FLY). The TEY measurement is sensitive to the surface and near surface regions of the sample, and the FLY is more sensitive to the bulk and is particularly useful for the nonconducting materials.

For light emitting samples, such as tris (8-hydroxyquinoline) aluminum (Alq_3) used in the organic light emitting diodes (OLEDs) and porous silicon, optical and electronic properties can be studied by the technique of x-ray excited optical luminescence (XEOL). XEOL is an x-ray photon in, optical photon out technique. The advantages of XEOL, using tunable soft x-ray synchrotron radiation as the excitation source, are its state and site selectivity.[1,2] The tunability of synchrotron radiation makes it possible to study XEOL of a particular element or even a specific chemical state in a composite environment. Soft x rays have a short one-absorption length ($\sim 10^2-10^3$ nm),[2,3] comparable to typical film thickness. In an XEOL experiment, the optical spectrum can be recorded at selected incident photon energies. Additionally, the XANES can be recorded in the photoluminescence yield (PLY).[4] When these three detection modes are collectively used to record the XANES, one could study the electronic and optical properties of samples in terms of sampling depth, with the TEY being the most surface sensitive, and the FLY the most bulk sensitive.

Here, we present some recent applications of the XEOL to the studies of three classes of light emitting materials: (a) porous silicon at the Si $L_{3,2}$ edge to illustrate the site and chemical selectivity of XEOL in distinguishing between photoluminescence from the quantum-confined porous silicon and the defected amorphous SiO_2;[5,6] (b) organic light emitting materials, such as Alq_3 and tris-(2,2′-bipyridine) ruthenium (II) $[Ru(bpy)_3^{2+}]$ at the C, N, and O K edges,[7,8] to determine their active luminescence sites; and (c) CdS nanoparticles at the S K edge to show the surface/bulk site specificity and chemical selectivity.[9]

II. EXPERIMENT

Alq_3 and $Ru(bpy)_3(ClO_4)_2$ were obtained commercially. Porous silicon samples were prepared electrochemically.[10] The dendrimer-stabilized cadmium sulfide nanoparticles were prepared based on the published procedures.[9,11]

All experiments were performed at the Canadian Synchrotron Radiation Facility, located at the Synchrotron Radiation Center, University Of Wisconsin-Madison. The Grasshopper beamline was used for the Si $L_{3,2}$-edge study; the Spherical Grating Monochromator beamline was used for the study of the C, N, and O K edges; and the Double Crystal Monochromator beamline (1.8–4 keV) was used for the S K edge of CdS nanoparticles. A $J-Y$ H100 monochromator coupled with a Hamamatsu 943-02 photomultiplier tube was used to record the optical photons.

III. RESULTS AND DISCUSSION

Porous silicon is a silicon nanostructure that produces intense visible photoluminescence at room temperature.[12] It is often covered with a layer of amorphous SiO_2 of which the defects also exhibit photoluminescence. To distinguish between these two, we show in Fig. 1 the XEOL of porous silicon excited with photon energies at the Si $L_{3,2}$ edge. The one-absorption-length of photons at the Si $L_{3,2}$ edge (~100 eV) is ~60 nm, this length is significantly less than the

[a]Electronic mail: yfhu@facstaff.wisc.edu

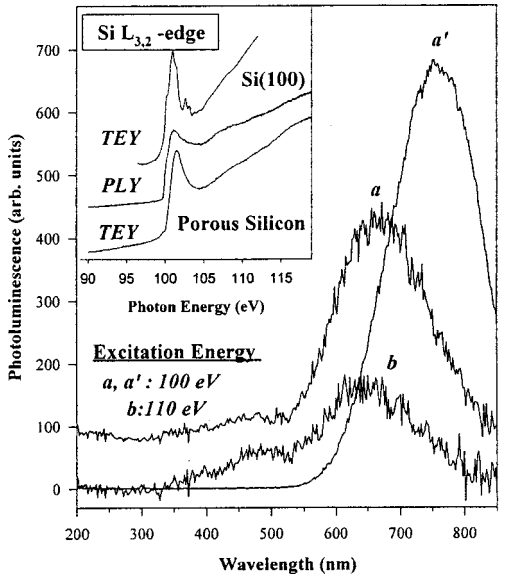

FIG. 1. Photoluminescence excited at: (a) 100 eV and (b) 110 eV from an as-prepared porous silicon. Luminescence of the HF refreshed porous silicon excited at 100 eV is shown as a'. XANES of the HF refreshed sample in TEY and PLY, and of the Si(100) in TEY, are also shown (inset).

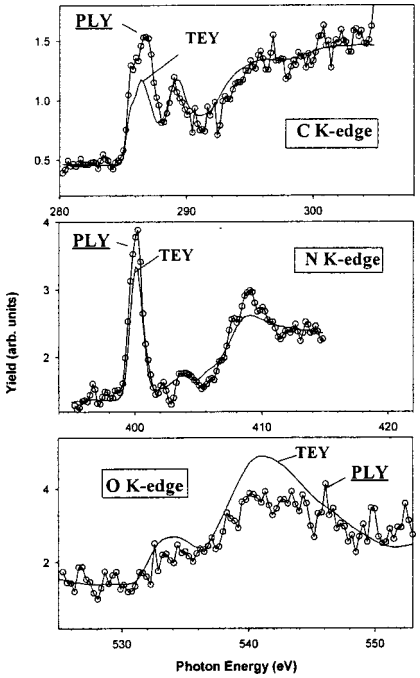

FIG. 2. XANES spectra of Alq_3 at the C, N, and O K edges, recorded in TEY and PLY modes.

thickness of porous silicon. We excited the specimen at (a) the elemental Si edge (100 eV) and (b) the SiO_2 resonance (110 eV). We see that there is an intense peak at about 650 nm and two satellites at 480 and 380 nm. The 650 nm peak is the most intense at 100 eV excitation. Its intensity decreases noticeably at 110 eV accompanied by an increase in the intensity of the satellites. This observation permits the assignment of the main peak at 650 nm as luminescence from the nanocrystallite silicon and the satellites from the surface oxide. Upon removal of the surface oxide with HF, the satellites disappear and the porous silicon peak is more intense and redshifted due to further etching and polishing.[2] Similar behavior has been observed at all core levels of Si.[5]

Alq_3 and $Ru(bpy)_3^{2+}$ are prototype chiral transition metal complexes. Because of its strong photochemical stability, and high luminescence efficiency (radiative recombination of holes and electrons in the valence and conduction band, respectively), Alq_3 has long been the key component in the OLED research,[13] and $Ru(bpy)_3^{2+}$ has also been used more recently in OLED devices.[14] XEOL can provide site selectivity to the study of electronic and optical properties and has shown promise in understanding the luminescence mechanism of these materials.[7,8,15]

Figure 2 shows the C, N, and O K-edge XANES spectra of Alq_3 recorded in TEY and PLY modes. The TEY has been normalized to the PLY for direct comparison. The sharp resonances around 286 eV at the C K edge are dipole transitions from the C $1s$ to lowest unoccupied molecular orbital (LUMO) and LUMO+1 etc. This doublet can be attributed to $1s$ to π^* transitions from the aromatic carbons, especially those farthest away from the N and O atoms. These features are enhanced noticeably in the PLY relative to the TEY while the intensities of other C K-edge XANES features at higher energy are similar to those of the TEY. The LUMO is directly populated by the transition, and associated Auger decay populates the highest occupied molecular orbital holes. This facilitates hole–electron recombination, hence luminescence. The higher energy features are transitions to σ^* states not involved in the chromophore π bonding.

The C and N K-edge XANES of $Ru(bpy)_3^{2+}$ in TEY, FLY, and PLY are shown in Fig. 3. Similar to the Alq_3 complex, the two peaks at 285.7 and 286.5 eV are C $1s$ to π^* dipole transitions of nonequivalent carbons on the bipyridine ring. The carbon atoms that are not adjacent to the electronegative N have different core level binding energy shifts, in good accord with the results of Alq_3. Peaks of the Ru $M_{5,4}$ edges ($3d_{5/3,3/2}$ to Ru $4p$ transitions) are expected at ~280 and 284 eV, respectively, but are not noticeable in TEY and FLY due to a smaller edge jump and absorption cross section of Ru $M_{5,4}$ edge relative to the C K edge. The most noticeable PLY feature is the suppression of the broad resonance at ~289 eV. This feature is associated with transition from $1s$ to σ^* quasibound states (not directly connected to the chromophore π ring) where the electron can tunnel out into the continuum suppressing luminescence. This observation again indicates that XEOL can be site and excitation channel specific.

In contrast to the PLY spectrum of Alq_3, Fig. 3(b) shows an inverted PLY XANES of the N K edge for $Ru(bpy)_3^{2+}$. Inversion in PLY is not uncommon in soft x-ray optical XANES when the specimen is thick (total absorption) as is the case here in the 280–430 eV absorption region, and all the elements are competing for all incoming photons. It should be noted that the difference in absorption coefficients below and above the N K edge is large for N but negligible for C, while the total number of photons is essentially the same. Thus, there is an abrupt change in the distribution of the fraction of photons absorbed by N and the rest of the system (mostly C) across the N K edge. A negative edge jump implies that N is less effective (lower quantum yield)

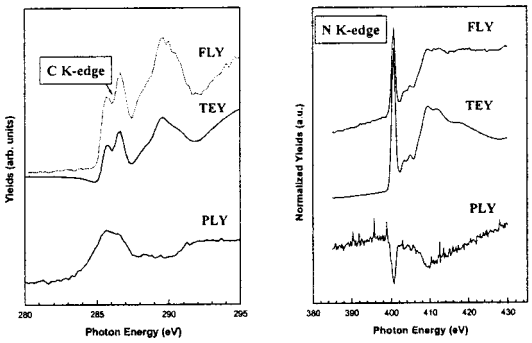

FIG. 3. C and N K edge XANES of $Ru(bpy)_3^{2+}$ in TEY, FLY, and PLY.

than C in producing luminescence per photon absorbed. In addition, the probing depth of PLY decreases at the intense N edge π^* resonance for a thick sample, resulting in a decrease in more effective luminescent sites (carbon) per photon absorbed, facilitating an inversion. Dendrimer-stabilized CdS quantum dot is another type of the nanomaterials that shows interesting blue-light emission.[11,16] Figure 4 shows the XEOL spectra of a specimen of 2 nm dendrimer-stabilized CdS nanoparticles, the surface of which was oxidized to sulfate SO_4^{2-}.[9] Spectra (a), (b), and (c) were excited with selected photon energies across the S K edge marked with vertical bars in the XANES (inset), collected in both the TEY and the PLY. We see that the luminescence intensity of the CdS nanoparticles was enhanced dramatically from (a), below the S K edge to (b), at the CdS S K edge white line, corresponding to the TEY. In contrast, the XEOL intensity with excitation energy (c), the S K-edge absorption at the white line resonance of SO_4^{2-}, was greatly suppressed relative to the TEY. This is apparent in the XANES (inset). The surface sensitive TEY spectrum shows two resonances at 2474 and 2480 eV, corresponding to transitions of S 1s to unoccupied orbitals in cadmium sulfide (CdS) and sulfate (SO_4^{2-}), respectively. However, the PLY only shows a dominant sulfide feature at 2474 eV. A comparison of the CdS nanoparticle PLY XANES with the TEY of bulk CdS shows that they are the same. Thus we can conclude that the luminescence originates mainly from the nano CdS.

IV. CONCLUSION

We have reported the XEOL study of three classes of light emitting materials. We showed that this technique can be used to investigate the luminescence mechanism in porous silicon, to show the site specificity, particularly in the aromatic ring C of the organic light emitting materials, and to understand the origin of the luminescence of CdS nanoparticles and to differentiate surface and bulk compositions of CdS nanoparticles. Finally, it should be noted that the site selectivity of XEOL could not always be obtained for any light emitting material. The interpretation of the XEOL (e.g., when there is an inverse in edge jump) can be sometimes difficult since the results depend somewhat on specimen

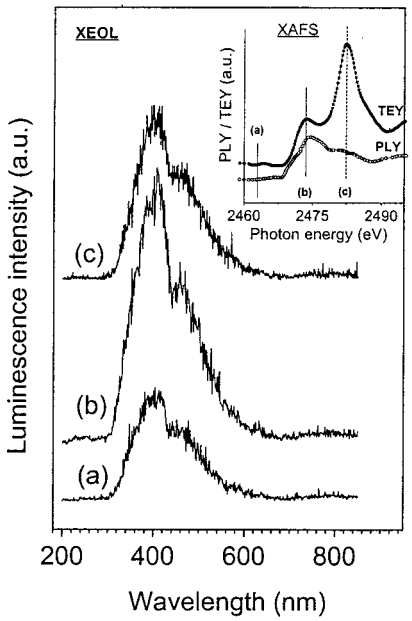

FIG. 4. Normalized XEOL spectra of nano-CdS excited with various x-ray energies across the S K edge. The inset shows the XANES in TEY and PLY and the corresponding excitation photon energies (vertical bars) for (a), (b), and (c).

preparation and experimental conditions. This is especially true in the case of hard x-ray excitation when the secondary processes play a more significant role in the production of the holes and electrons.[1] However, this problem is more manageable in the soft x-ray region.[2]

ACKNOWLEDGMENTS

This work is financially supported by the Natural Sciences and Engineering Research Council (NSERC) of Canada. The work was performed at CSRF, located at SRC, University of Wisconsin-Madison which is supported by the National Science Foundation under Grant No. DMR-0084402.

[1] A. Rogalev and J. Goulon, in *Chemical Applications of Synchrotron Radiation*, edited by T. K. Sham (World Scientific, Singapore, 2001).
[2] T. K. Sham, S. J. Naftel, and I. Coulthard, in *Chemical Applications of Synchrotron, Radiation*, edited by T. K. Sham (World Scientific, Singapore, 2001).
[3] *X-ray Data Booklet* (Center for X-ray Optics, Lawrence Berkeley National Laboratory, UC-Berkeley, 2001); website at:http://www-cxro.lbl.gov/.
[4] T. Murata *et al.*, Jpn. J. Appl. Phys., Part 1 **C20**, 213 (1993).
[5] S. J. Naftel *et al.*, Phys. Status Solidi A **182**, 373 (2000).
[6] T. K. Sham *et al.*, Nature (London) **363**, 331 (1993).
[7] S. J. Naftel *et al.*, Appl. Phys. Lett. **78**, 1847 (2000).
[8] P. S. Kim *et al.*, J. Am. Chem. Soc. **123**, 8870 (2001).
[9] P. Zhang, S. J. Naftel, and T. K. Sham, J. Appl. Phys. **90**, 2755 (2001).
[10] F. Koch, V. Petrova-Koch, and T. Muschik, J. Lumin. **57**, 271 (1993).
[11] K. Sooklal *et al.*, Adv. Mater. **10**, 1083 (1998).
[12] A. G. Cullis *et al.*, J. Appl. Phys. **82**, 909 (1997).
[13] C. W. Tang and S. A. Van Slyke, Appl. Phys. Lett. **51**, 913 (1987).
[14] F. G. Gao and A. J. Bard, J. Am. Chem. Soc. **122**, 7416 (2000).
[15] T. K. Sham *et al.*, Thin Solid Films **363**, 318 (2000).
[16] J. R. Lakowicz *et al.*, J. Phys. Chem. B **103**, 7613 (1999).